Contents

ASM J. Sc.
vol. 1, no. 1, 2007

ISSN 1823-6782

MOSTI

AKADEMI SAINS MALAYSIA

ASM Science JOURNAL

In Pursuit of Excellence in Science

Vol. 1. No 1. June 2007 • ISSN : 1823-6782

ASM JOURNAL Science

INTERNATIONAL ADVISORY BOARD

Ahmed Zewail (Nobel Laureate)
Richard R. Ernst (Nobel Laureate)
John Sheppard Mckenzie
M.S. Swaminathan

EDITORIAL BOARD

Editor-in-Chief/Chairman: Mazlan Othman

Abdul Latiff Mohamed
Chia Swee Ping
Ibrahim Komoo
Lam Sai Kit
Lee Chnoong Kheng
Looi Lai Meng
Mashkuri Yaacob
Md. Ikram Mohd Said
Mohd Ali Hashim
Francis Ng
Radin Omar Radin Sohadi

Editorial

The *ASM Science Journal* (*ASM Sc. J.*) is intended to be one of the primary vehicles of the Academy of Sciences Malaysia to stimulate and nurture excellence in science and technology for the development of the nation and for the benefit of mankind. Its purpose is also to widely disseminate significant research developments and deliberate on R&D strategies and policies. It will further provide a major opportunity for showcasing the effectiveness of scientific and technical efforts and increasing the efficiency of management of research and development which is linked with the ability to communicate information about current research efforts and the results of past work. This journal will pay attention to the importance of scientific and technical endeavour and contribute to the better understanding of problems of science and technology through its regular publication and wide circulation, thus promoting cooperation and exchange of views among the science community worldwide. All these objectives are fully in line with the aims and objectives of the Academy.

In this maiden issue, there are contributions from many fields covering both fundamental and applied research: medicine, engineering, chemistry, electronics, mechanics and physics. Our future plan is to gear one issue a year towards a particular theme. The papers in that issue will address current and impending issues, and the demands and needs of the scientific community and society pertaining to the selected theme.

It is hoped that this varied, vital and vigorous exchange of scientific information that the Journal provides will assist in better understanding the various forces and factors that affect the progress of humanity and safeguard its survival. The Academy of Sciences Malaysia, therefore, in earnestly discharging its responsibility, proudly associates itself with this Journal in striving to promote an international exchange of scientific information.

Mazlan Othman
Editor-in-Chief/Chairman, Editorial Board *ASM Sc. J.*

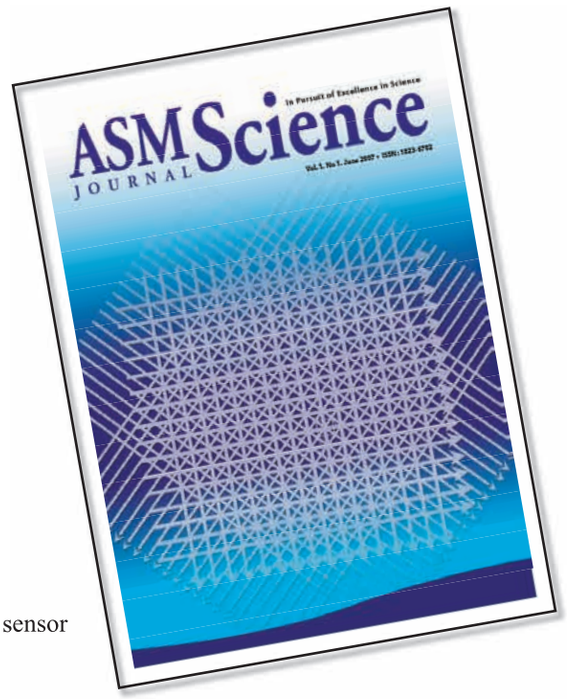

Cover:
Optical tomography sensor projection geometry
(Article: p. 27)

publication(latest).indd 1 13/2/08 11:21:28 AM

ASM Sci. J., **1(1)**, 27–36

Optical Tomography: Real Time Image Reconstruction for Various Flow Regimes in Gravity Flow Conveyor

R. Abdul Rahim[1*], J. F. Pang[1], K. S. Chan[1], L. C. Leong[1] and M. H. Fazalul Rahiman[2]

In this study, real-time imaging was monitored for flowing solid particles when various baffles were created to block certain areas of the pipe. The generated flow regimes were full-flow, three-quarter-flow, half-flow and quarter-flow. A vertical pneumatic conveyor was designed to hold a 85 mm inner diameter pipeline. The four projection optical tomography systems used, applied the parallel beam projection approach and use infrared light sources so that the sensor was free of noise from the surrounding visible light source. The two orthogonal and two rectilinear projections were axial, but ideally they should have been in the same layer. The sensor readings could be related to the varying light intensity effects of the dropping particles and were used to provide cross-sectional distribution information for the conveyor. By using computer programming, the information was reconstructed to produce coloured images and concentration was obtained by reference to a colour code. The results obtained from this study showed how imaged flow followed the artificial flow regime. This study could benefit industrial production lines in maintaining the desired flow rates.

Key words: pneumatic conveyor; pipeline; optical tomography; computer programming; flow imaging; infrared light sensor; material packaging

Tomography is an imaging technique that produces high-resolution cross-sectional images of the internal structure of an object (Cruz 2003). In the processing industry, information describing material distribution and validating internal modes of the process are necessary for optimum design and operation of process equipment (Ruzairi 1996). Hence, the tomography approach using non-invasive sensors is a novel and safe way to visualize the inside of a mixing vessel. Some flow information can be obtained uniquely through process tomography, for example the local concentration, velocity of movement, flow rate, composition of flow and others. Optical tomography is an attractive method since it may prove to be less expensive, have a better dynamic response, and be more portable for routine use in process plants compared to other radiation-based tomographic techniques, such as positron emission, nuclear magnetic resonance, gamma photon emission and X-ray tomography (Chan & Ruzairi 2002). Process tomography provides several real-time methods (Cruz Meneses-Fabian *et al.* 2003) to obtain cross-section parameters in process plants related to material distribution. These methods involve taking numerous measurements from sensors placed around the vessel of the investigated process plant. The measured data are then fed into a computer program to obtain the internal behaviours of the conveyor.

Generally, vertical pneumatic conveying is defined as the transport of various granular solids and dry powders using air or other inert gas stream as a transportation medium in gravity flow. Nowadays, material handling by pneumatic conveying is increasingly becoming routine in industrial businesses. Pneumatic conveying offers many advantages over other methods of granular solids transport such as low routine maintenance and manpower costs, dust-free transportation and flexible routing. Some of the applications of pneumatic conveying systems can be found in industries dealing with food processing, plastic product manufacturing, textile, paper, power generation and solids waste treatments (Arko 1999).

Sensor Configuration

In optical tomography, there are many types of projection patterns used to detect flow material within pipelines. Basically, they can be divided into groups of parallel beam projections and fan beam projections. As mentioned earlier, this study uses the first approach. The parallel beam projection is obtained through the parallel arrangement of several transmitter sensors and the view angle of each receiver sensor is designed to be small. Four parallel beam projections result in patterns of two orthogonal projections, two rectilinear projections, combination of

[1] Process Tomography Research Group, Control and Instrumentation Engineering Department, Faculty of Electrical Engineering, Universiti Teknologi Malaysia, 81310 UTM Skudai, Johor, Malaysia

[2] Department of Mechatronics Engineering, North Engineering College University, Universiti Teknologi Malaysia, 81310 UTM Skudai, Johor, Malaysia

* Corresponding author (e-mail: ruzairi@.fke.utm.my; ruzairiabdulrahim@yahoo.co.uk)

one orthogonal with two rectilinear projections and combination of two orthogonal with two rectilinear projections (Sallehuddin 2000). This latter arrangement can provide sufficient information to minimize ambiguous effects arising during cross-sectional image detection compared to the previous three projections.

In the two orthogonal projections, there were two arrays of projections. Both have their viewing planes parallel to the horizontal axis of the vertical flow pipe; the two arrays are at 90º to each other. In this project, each orthogonal array used 16 pairs of transmitter-receiver and this resulted in a true image resolution of 16 × 16 pixels. For the two rectilinear projections, the arrays of projections were inclined at plus and minus 45º to the horizontal axis respectively. The number of transmitter-receiver pairs used in one array was 23, because each emitter projection in this layer must cross over the center point of the corresponding pixel and also the area within the pipeline, as shown in Figure 1. The hardware resolution in this project doubled the resolution obtained from the previous research conducted by Sallehuddin *et al*. (2000) that used 8 × 8 pairs of transmitter-receivers, in the layer of two orthogonal projections and 11 × 11 pairs of transmitter-receivers in the layer of two rectilinear projections.

A typical optical tomography system consists of a sensor, an electronic circuit, a data acquisition system, and a host computer as the data processing and display unit. The block diagram of the developed system is shown in Figure 2. A transmitter circuit sequentially switches on the emitter lights and projects them to receivers. The signal conditioning circuit then converts the signals received into voltage readings and amplifies them to a sufficient level. Finally, the output signals pass through a sample and hold the circuit to the analogue switching circuit and the data

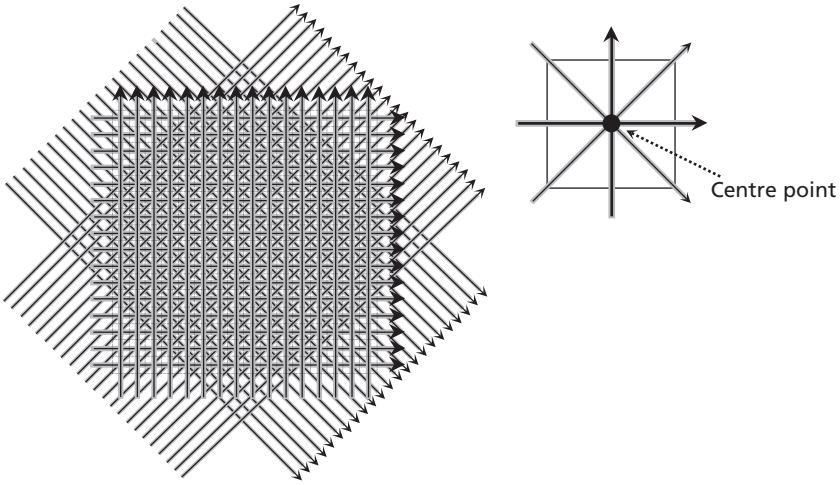

Figure 1. Optical tomography sensor projection geometry.

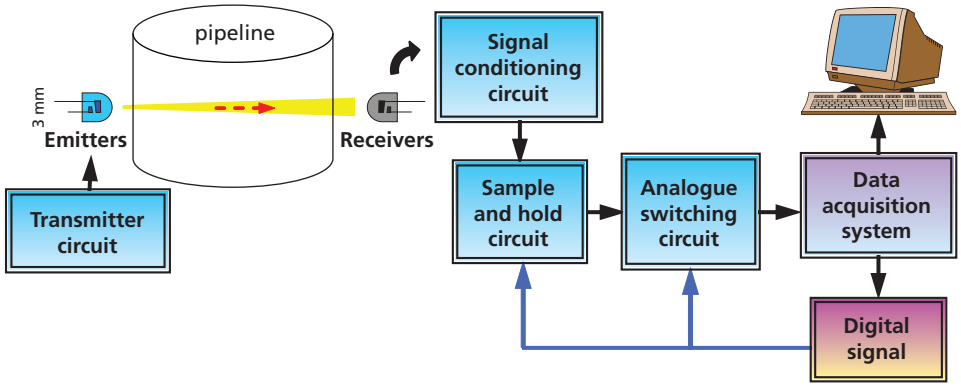

Figure 2. Block diagram of the developed system.

acquisition system based on the control signals from the digital signal controller. The data acquisition system digitises the signals and passes them into the computer for further processing.

A fixture was designed for holding all emitters and receivers so that four parallel projection arrays could be created easily. The two orthogonal projections and two rectilinear projections are ideally in the same layer. Practically, if all projections were in one layer, three main problems would occur. Firstly, light from the emitters travelled a longer distance to reach the receivers since the inner diameter of the pipe used in the system was already at 85 mm. This meant that the emitter itself should have a higher light intensity capability. Unfortunately, for the emitter that had a higher intensity, the physical size was greater than 3 mm in diameter and also the cost was higher. Secondly, the developed fixture would look bulky. Thirdly, since the radiant intensity of the emitter was proportional to the forward current used, the power consumed for the whole system would increase. Thus, the fixture was constructed using two layers as shown in Figure 3. The upper layer was for two rectilinear projections and contained 92 holes in total, 23 holes per side. The lower layer was for two orthogonal projections and it contained 64 holes in total, 16 holes per side. The distance between these two layers was 7 mm to provide mechanical stability.

It is essential for the beam of light to diverge as little as possible to avoid overlapping of the received signals and loss of beam intensity (Ruzairi 1996). Three methods were used to collimate the light source. Firstly, infrared emitters and phototransistors that had small view angles were used. Secondly, an optical stop was placed in front of the infrared emitter. In this system, a ferrule was used as the stop. This method is effective in limiting the divergent angle (Chan 2001). The stop was 1 mm in diameter and it successfully limited the light from the 3 mm infrared emitter as shown in Figure 4. Thirdly, all emitters and receivers were arranged in an alternate manner as shown in Figure 4. This arrangement helps to cut down any divergent light reaching receivers adjacent to the designated receiver.

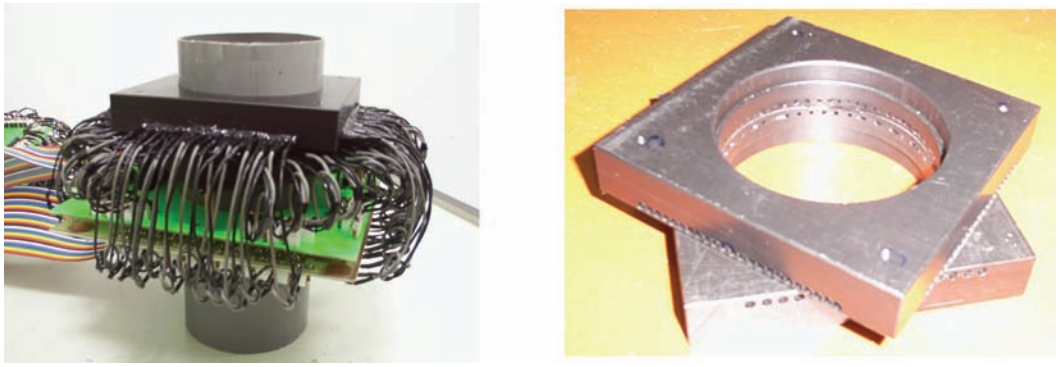

Figure 3. Fixture for holding emitters and receivers.

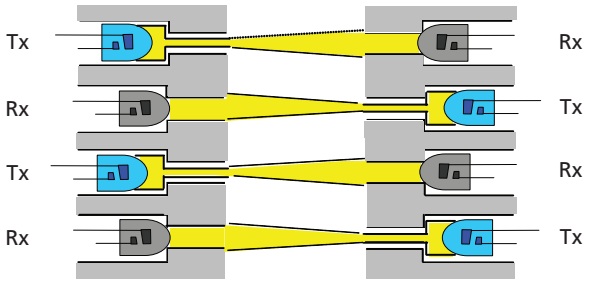

Figure 4. Optical stopper and alternate arrangement of emitters and receivers.

Concentration Profile

The concentration profile is the result obtained from the concentration measurements. The profile is generated when all corresponding sensor readings are applied into an algorithm, namely the image reconstruction algorithm. There are many different algorithms, e.g. Linear Back Projection (LBP), Filtered Back Projection, Convolution Back Projection, Hybrid Reconstruction Algorithm (HRA) and Algebraic Reconstruction Technique. For this project, the HRA was chosen since it can improve the accuracy of the image reconstruction obtained using LBP by neglecting the blurry image. According to Sallehuddin (2000), this algorithm assumes binary values from the sensor, either zero for no material or one for the presence of material. The sensor value is first measured, if the reading is zero, then any pixels traversed by that sensor's beam are set to zero and omitted from further calculations. Only the rest of the pixels will perform LBP to complete the process. In other words, this algorithm can be easily explained as a make up or packing of the LBP algorithm with several masking conditions. The mathematical expression of this algorithm is shown below:

$$V_{\text{Hybrid}}(x_{sa}, y_{sb}) = \begin{cases} V_{Sa} - V_{\text{th}} + V_{Sb} - V_{\text{th}}; \\ \quad V_{Sa} \geq V_{\text{th}} \text{ AND } V_{Sb} \geq V_{\text{th}} \text{ AND} \\ \quad V_{Sc} \geq V_{\text{Sp}} \text{ AND } V_{Sd} \geq V_{\text{Sp}} \\ 0; V_{Sa} < V_{\text{th}} \text{ OR } V_{Sb} < V_{\text{th}} \text{ OR} \\ \quad V_{Sc} < V_{\text{Sp}} \text{ OR } V_{Sd} < V_{\text{Sp}} \end{cases} \quad (1)$$

where V_{hybrid} (x_{sa}, y_{sb}) is the voltage of pixel (x_{sa}, y_{sb}) inside the concentration profile using the Hybrid image reconstruction algorithm; V_{Sa} or V_{Sb} is the voltage value referring to the sensor S_a or S_b in two orthogonal projections (also called the 16 × 16 layer). V_{Sc} or V_{Sd} is the voltage value referring to the sensor S_c or S_d in two rectilinear projections (also called the 23 × 23 layer); a is the sensor number between 0 to 15 in the first 16 × 16 layer projection, b is the sensor number between 16 to 31 in the orthogonal 16 × 16 layer projection, c is the sensor number between 0 to 22 in the first 23 × 23 layer projection, d is the sensor number between 23 to 45 in the orthogonal 23 × 23 layer. V_{th} is threshold voltage of the 16 × 16 layer and V_{sp} is threshold voltage of the 23 × 23 layer. When an obstacle, for example, passes through the sensing field, the concentration profile obtained by applying Equation 1 is illustrated in Figure 5.

Experimental Flow Rig Setup

The flow rig is designed to create the continuous gravity flow of plastic beads. The configuration of the flow rig is illustrated in Figure 6. It consisted of a hopper, a valve, two gaps, a space for the arrays of tomographic sensors, a tank and a blower. The blower conveys the plastic beads from the tank to the hopper; the valve is a switch to open or close the hopper to ensure that the plastic beads flowing inside the pipe could drop down or be obstructed. Two gaps near to the hopper were filled with the corresponding cut-off blades for controlling the

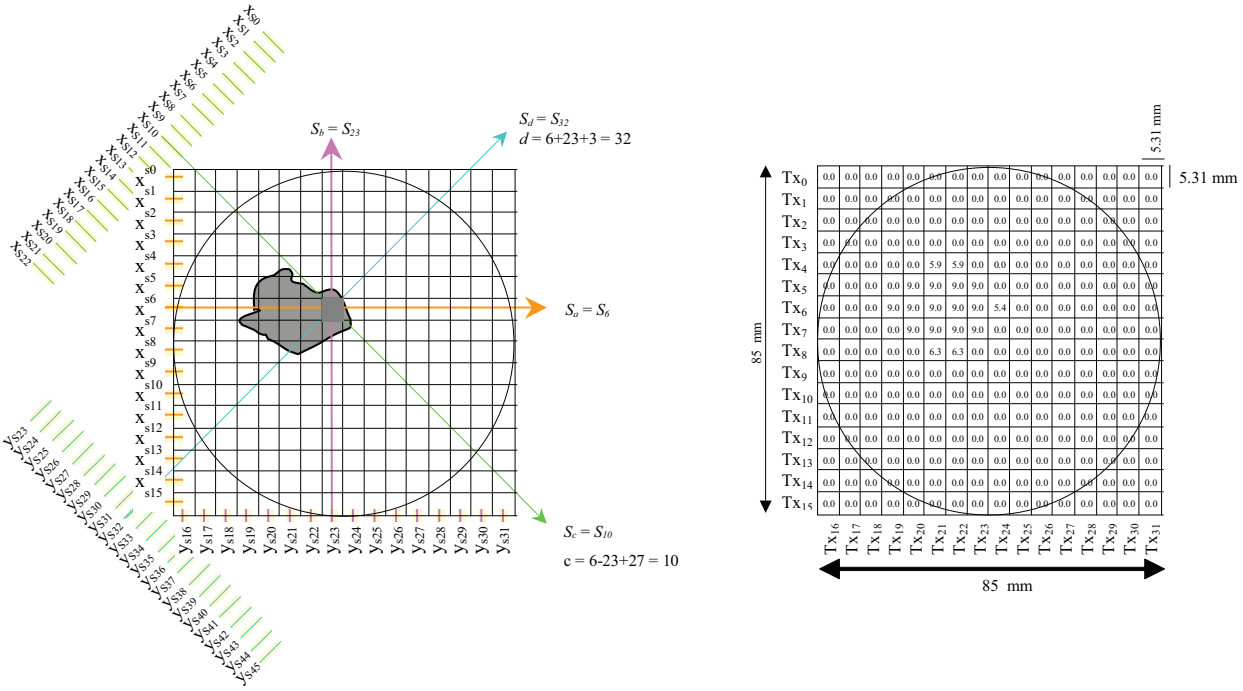

Figure 5. Concentration profile of detected obstacle.

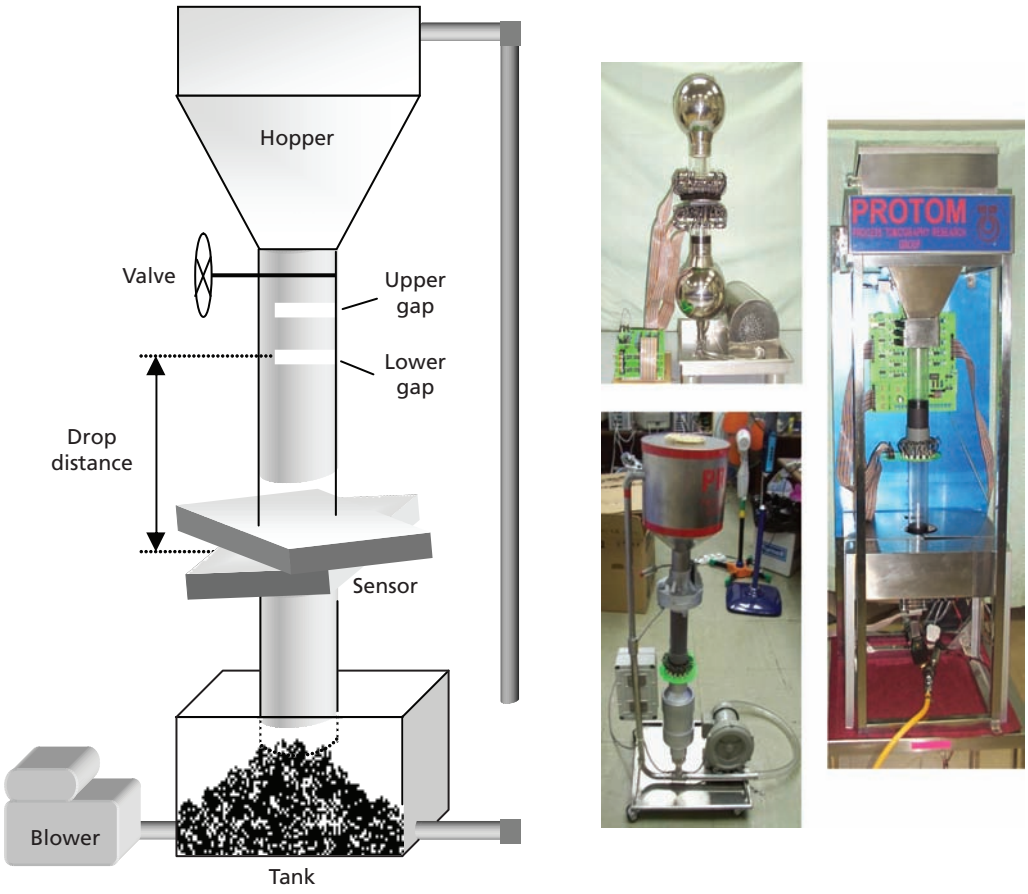

Figure 6. Vertical flow rig configuration.

mass flow rate and flow regime. The upper gap was located 3 cm below the valve and the lower gap at 8 cm from the upper gap. The pipeline of the flow rig had an inner diameter of 85 mm. The plastic beads used in the flow rig had a volume of approximately $2 \times 2 \times 3$ mm^3. It was very light (less than 1 g) and also of a pure material that could be used in the manufacturing industry.

Designation of artificial flow regime. Four artificial flow regimes were investigated: full-flow, three-quarter flow, half-flow and quarter-flow (Ruzairi 1996). They were created by placing the corresponding cut-off blade or baffle into the lower gap of the flow rig. In the full-flow regime, no baffle was created to block the flow. The flow expectation is shown in Figure 7.

In the three-quarter-flow regime, the designed baffle cuts-off was at a quarter of the area of pipeline, thus three quarters were clear for plastic bead flow. The three-quarter flow expectation in the pneumatic conveyor is illustrated in Figure 8.

In the half-flow regime, the designed baffle cut off half the area of the pipeline leaving the half clear for the plastic beads to flow. The half-flow expectation in the conveyor is shown in Figure 9.

In the quarter-flow regime, the designed baffle cut off three quarters of the area of the pipeline, thus only a quarter was clear for the flow of the plastic beads. The quarter-flow expectation is illustrated in Figure 10.

Mass flow rate controlling baffle. Three experimental mass flow rates were created by placing the corresponding cut-off blade in the upper gap of the flow rig. The configuration of the three baffles are shown in Figure 11. The cut-off regions of these baffles were circular with diameters of 4.5 cm, 4 cm and 3.5 cm respectively. They fix and maintain the corresponding mass flow rate.

RESULTS AND DISCUSSION

To construct real time cross-sectional images of different flow regimes, the corresponding flow rate control baffle and flow regime baffle were first placed into the appropriate gaps of the conveyor. When the measurement process was in running phase, a total of 78 sensor output readings were

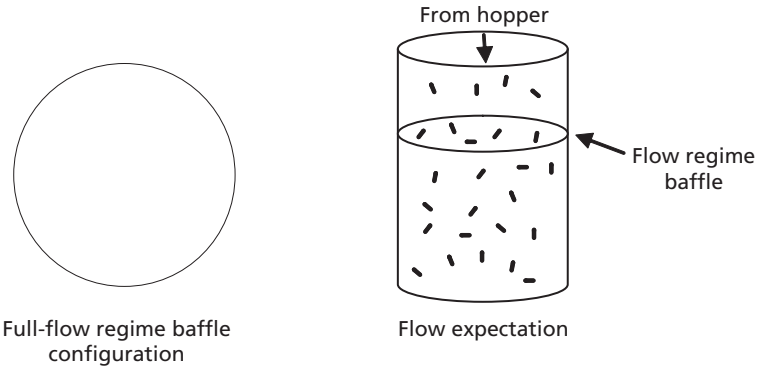

Figure 7. Full-flow regime creation.

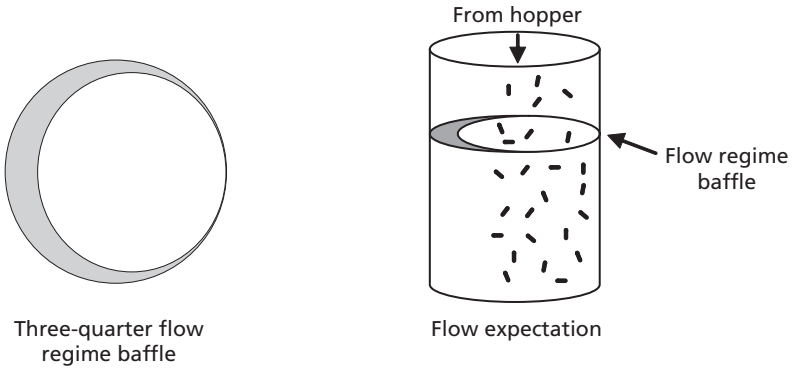

Figure 8. Three-quarter flow regime creation.

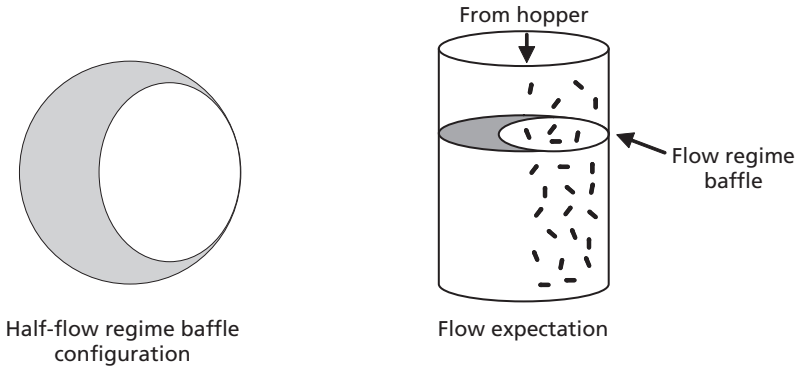

Figure 9. Half-flow regime creation.

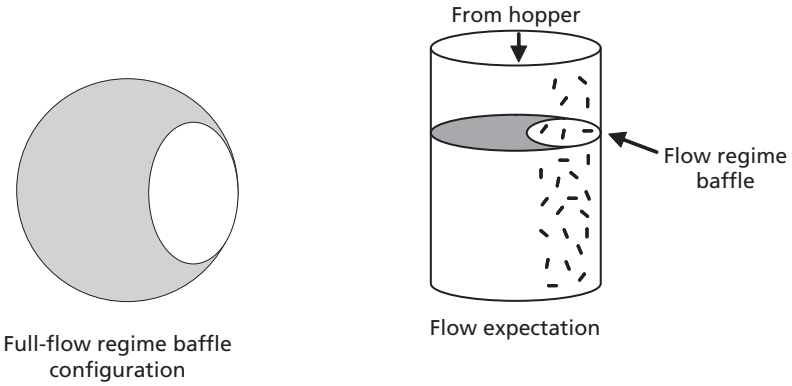

Figure 10. Quarter-flow regime creation.

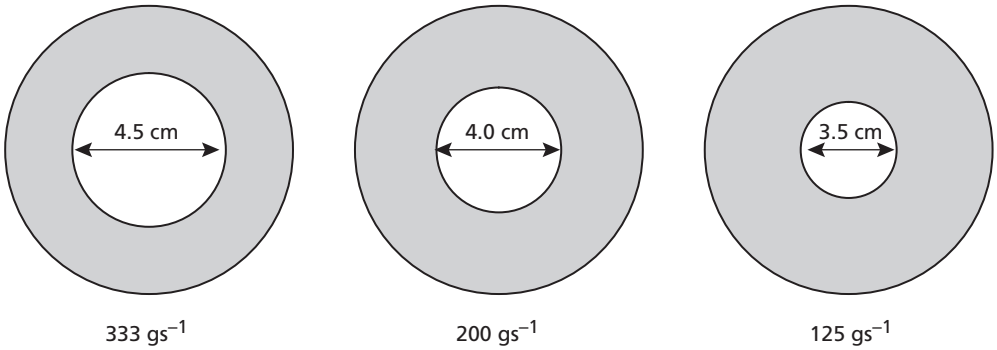

Figure 11. Baffle configurations for controlling mass flow rate.

captured by the data acquisition system for each frame of process. After applying the hybrid reconstruction algorithm or Equation 1, the concentration profile was generated with a resolution of 16 × 16 pixels. By referring to a colour code showing the % ratio of light absorbed by the sensor (100% means the obstacle was fully blocking the light transmitted), the concentration profile detected, was converted to the flow image with a resolution of 16 × 16 pixels. If filtering and image interpolation methods were used, the generated cross-sectional image could be upgraded into the high resolution image shown in Figure 12.

In the concentration measurement, the measured cross-sectional images were made at three different drop distances, these were from 16 cm, 36 cm and 56 cm, respectively (Figure 6). This was done by relocating the tomographic sensor array's position relative to the lower gap of the pneumatic conveyor. The results obtained are illustrated in Figure 13.

The results showed that the images for the drop distance of 16 cm had a higher concentration compared to the drop distances of 36 cm and 56 cm. When flow passed

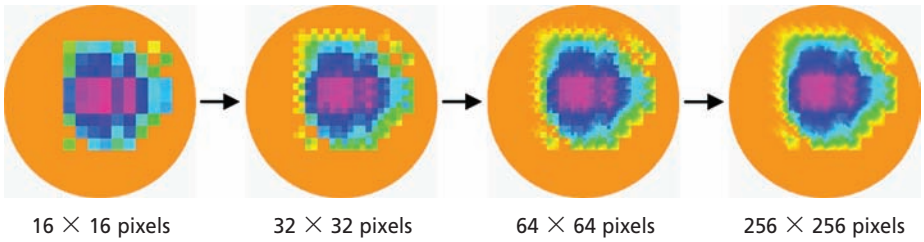

Figure 12. Upgrading original image resolution to higher resolution.

through a long distance in gravity flow, it is affected by the velocity, wall friction and collision among the particles. These factors make the flow of particles less predictable and they are scattered and more randomly distributed within the pipeline. This is demonstrated by observing the half-flow and quarter-flow regimes at the flow rate of 333 gram/s, and comparing them with the cross-sectional images constructed at the drop distance of 56 cm where the flow is fairly uniformly distributed and unable to follow the required regime.

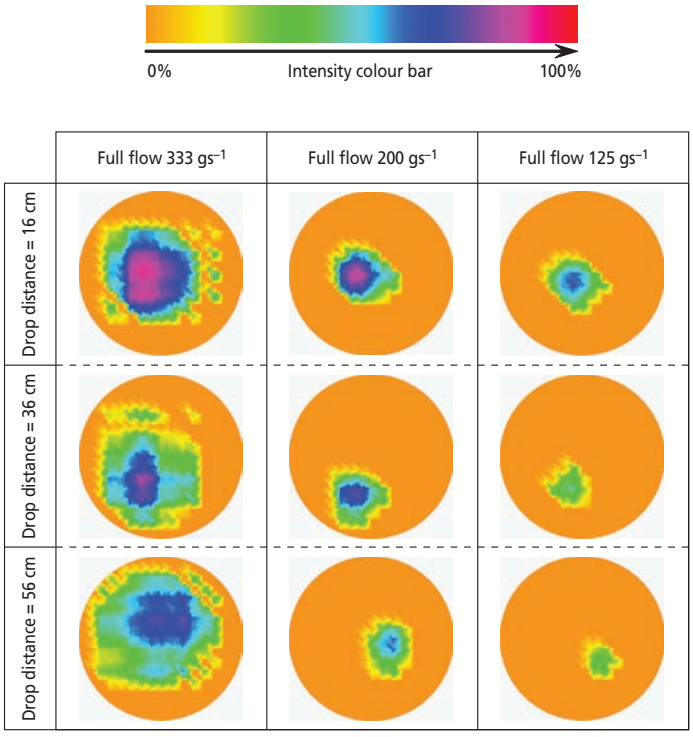

(a) Full-flow regime

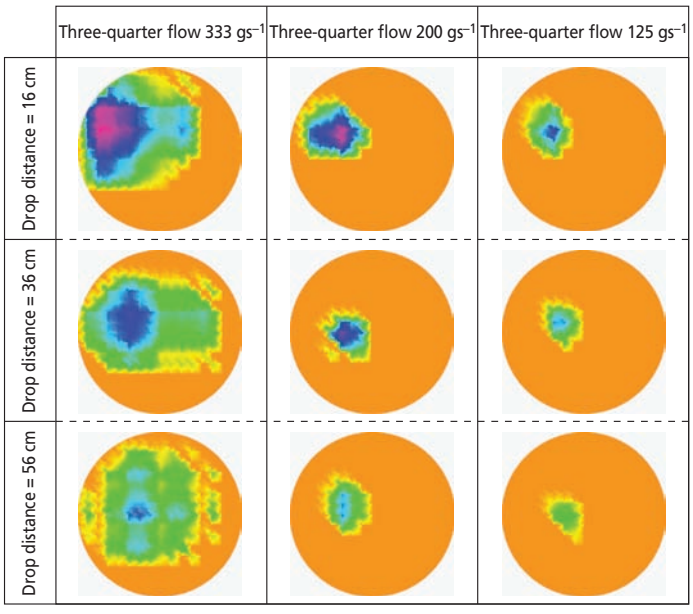

(b) Three-quarter flow regime

Figure 13. Cross-sectional images of various flow regimes.

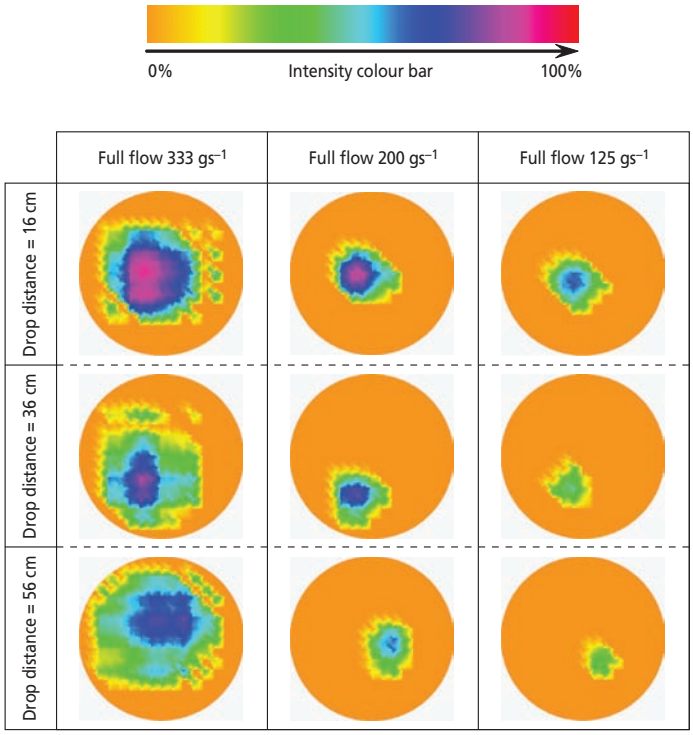

(c) Half-flow regime

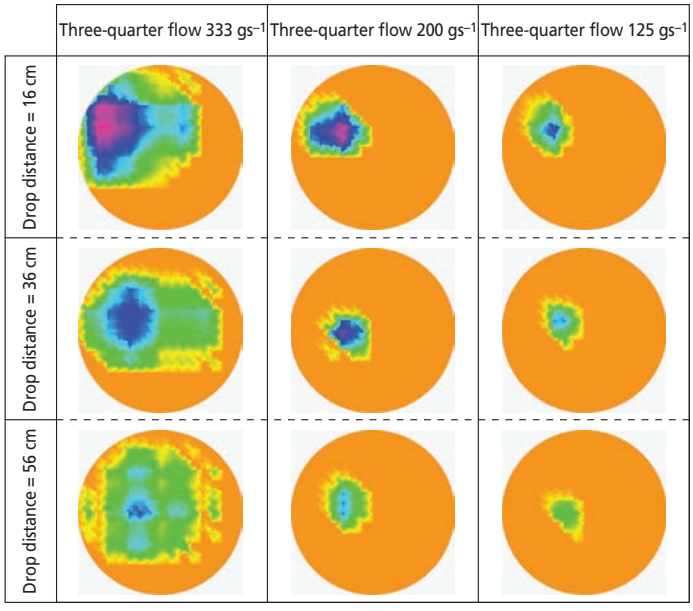

(d) Quarter-flow regime

Figure 13 cont. Cross-sectional images of various flow regimes.

CONCLUSION

Image reconstruction was conducted for four different flow regimes (full-flow, three-quarter flow, half-flow and quarter-flow) in three mass flow rates with drop distances of 16 cm, 36 cm and 56 cm. It could be concluded that at the longest drop distance used, fewer of the plastic beads followed the required flow regimes. This was because collisions made the plastic beads deviate from the original flow. It also showed that the developed system was capable of showing the concentration profile of the flow.

An optical tomography system and the gravity pneumatic conveyor could have applications in industrial solid material handling and facilitate material control in a pre-mixing phase. The mass flow rate is a valuable parameter to be measured to control the flow. The proposed more recent method of using optical tomographic techniques to measure mass flow rate by integrating flow concentration, flow velocity and density of flow material together was investigated. This project provided the important points to be considered when undertaking flow velocity measurement and the velocity result obtained was of sufficient accuracy for computation of mass flow rate.

Date of submission: September 2006
Date of acceptance: May 2007

REFERENCES

Arko A, Waterfall RC, Beck MS, Dyakowski T, Sutcliffe, P & Byars, M 1999, 'Development of electrical capacitance tomography for solids mass flow measurement and control of pneumatic conveying systems', *Proceedings 1st World Congress on Industrial Process Tomography,* 14–17 April, Buxton, Greater Manchester, pp. 140–146.

Chan, KS 2001, 'Image reconstruction for optical tomography', B.Sc. dissertation, Universiti Teknologi Malaysia'.

Chan, KS & Ruzairi Abdul Rahim 2002, 'Tomographic imaging of pneumatic conveyor using optical sensor', paper presented at the World Engineering Congress, Sarawak, Malaysia, IEEE.

Cruz Meneses-Fabian, Gustavo Rodriguez-Zurita, Ramon Rodriguez-Vera & Jose F. Vazquez-Castillo 2003, 'Optical tomography with parallel projection differences and electronic speckle pattern interferometry', *Optics Communications,* vol. 228, pp. 201–210.

Ibrahim S, Green, RG, Evans, K, Dutton, K & Abdul Rahim, R 2000, 'Optical tomography for process measurement and control', paper presented at the *Control 2000*, UKACC International Conference, University of Cambridge, 4–7 Sept.

Ruzairi Abdul Rahim 1996, 'A tomography imaging system for pneumatic conveyors using optical fibres', PhD. thesis, Sheffield Hallam University, UK.

Sallehuddin Ibrahim 2000, 'Measurement of gas bubbles in a vertical water column using optical tomography', PhD. thesis, Sheffield Hallam University', UK.

Sallehuddin Ibrahim, Green, RG, Dutton, K & Ruzairi Abdul Rahim 2000, 'Modelling to optimize the design of optical tomography systems for process measurement', paper presented at *WARSAW 2000,* T-14.

ASM Sci. J., **1(1)**, 37– 41

Purification of Metallurgical Grade Silicon by Acid Leaching

V. A. Lashgari[1*] and H. Yoozbashizadeh[2]

Silicon, as the most important electronic material, has a lot of applications in the electronic industry and this includes the use of silicon in solar cells. One of the solar grade silicon production processes is the use of acid leaching for the removal of metallic impurities from silicon. The main advantage of this process for silicon purification is that it is based on a low temperature process. The purification of metallurgical grade silicon by acid leaching was studied as a function of time, temperature and etching. Based upon experimental results and under optimum conditions, it was possible to remove 41%, 71% and 25% of iron, calcium and aluminum respectively, with the use of aqua regia.

Key words: Metallurgical grade silicon; refining; solar grade silicon; acid leaching

At present, due to the use of clean and inexhaustible energy sources such as solar energy and the high demand of silicon for solar cells, much effort has been made to produce low cost pure silicon (Morita & Miki 2003, p.1111). It is known that the chlorosilane process (conversion of silicon to chlorosilanes, chlorosilanes purification by distillation and other means and reduction of chlorosilane in chemical vapour deposition reactors) is a highly complicated and costly process. Thus in recent years, research activities have been carried out on alternative methods to purify silicon, especially for solar cells of a lower purity level rather than those for semiconductors (Lian *et al.* 1992, p. 269). One of the improved methods to enhance silicon quality is the hydrometallurgical refining process which is termed acid leaching (Dietl 1983, p. 145).

The large diversity of experimental conditions and results, frequently contradictory, clearly illustrate the fact that the different types of metallurgical grade silicon (MG-Si) from different origins have different leaching behaviour. Hunt *et al.* (1976, p. 200) reported the removal of more than 90% of the impurities in MG-Si by leaching with aqua regia for 12 h at 75ºC. Dietl (1983, p. 145) reported that the best purification results were obtained using hydrochloric acid and hydrofluoric acid mixtures and finely ground MG-Si. Norman *et al.* (1985, p. 859) obtained 99.9% Si by leaching in three successive steps with aqua regia, hydrofluoric and hydrochloric acid.

In comparison to the structural composition, the size of particles or the leaching system seem unimportant to the final leaching yield. The choice of the correct phase structure makes it possible to work with coarser particles and obtain greater purification using less aggressive leaching systems. From these observations, controlling the alloy composition during solidification is very important for the removal of metallic impurities from silicon (Margarido *et al.* 1993, p. 1).

To remove all the harmful impurities from silicon, a combination of several refining processes will be needed. This is because of the different behaviour and their characteristics of the various impurities present (Morita & Miki 2003, p. 1111).

IMPURITIES IN MG-SI AND REFINING PROCESS

Carbothermic reduction of quartzite at high temperature arc furnace yields silicon with a purity of 98% (MG-Si) which is used for metallurgical applications as a deoxidizer and alloying element (Habashi 1997). Molten silicon from the arc furnace is cast into ingots. Table 1 represents the segregation coefficients of impurity elements in silicon. During solidification, elements with low segregation coefficients and concentrations higher than maximum solid solubility are precipitated along grain boundaries. When MG-silicon is ground and subjected to acid leaching process, the impurities are exposed to acidic agents (Santos *et al.* 1990, p. 237).

In Figure, 1 solid solubilities of impurity elements with temperature in silicon are presented. In most cases the maximum solubility occurs at around 1300ºC and are retrograde in behaviour both for lower temperatures and for temperatures nearer melting point (Dietl 1983, p. 145).

[1] School of Materials and Mineral Resources Engineering, Universiti Sains Malaysia, Engineering Campus, 14300 Nibong Tebal, Penang, Malaysia
[2] Department of Material Science and Engineering, Centre of Excellence in Advanced Materials, Sharif University of Technology, Tehran, Iran
* Corresponding author (e-mail: lashgari_v@hotmail.com.)

Table 1. Segregation coefficient of impurities in silicon.[a]

Impurity	Segregation coefficient
B	$8.00^{*}10^{-1}$
P	$3.50^{*}10^{-1}$
C	$5.00^{*}10^{-2}$
A1	$2.80^{*}10^{-3}$
Fe	$6.40^{*}10^{-6}$
Ti	$2.00^{*}10^{-6}$
Cu	$8.00^{*}10^{-4}$

[a] Morita & Miki 2003, p. 1111

Figure 2 demonstrates the attractiveness of hydrometallurgical purification. The lower the solid solubility, the lower is the value of the corresponding segregation coefficient (Dietl 1983, p.145).

EXPERIMENTAL PROCEDURE FOR REFINING PROCESS

The chemical analysis of silicon is shown in Table 2. The atomic absorption method (by HF-HNO3 acid digestion, HCl leaching and AAS) was used to determine the amount of metallic impurities. The results showed that, acid leaching was unable to remove impurities such as boron and phosphorus; however the main metallic impurities (Fe, Ca and Al) were effectively removed. After ballmilling, the silicon sample was sieved and a fraction with an average size under 100 μm was selected. Experiments were carried out in glass vessels with constant stirring and the temperature was controlled thermostatically.

Table 2. Chemical analysis of MG–silicon.

Element	Concentration (ppm)
Si	96%–98%
Fe	3150
Ca	70
A1	60
K	44
Mn	42
Mg	21

RESULTS

The influence of increasing the leaching time of aqua regia on the removal of impurities is illustrated for the three main impurities in Figure 3. Samples were leached with aqua regia at 50ºC and with a liquid:solid ratio of 10:1.

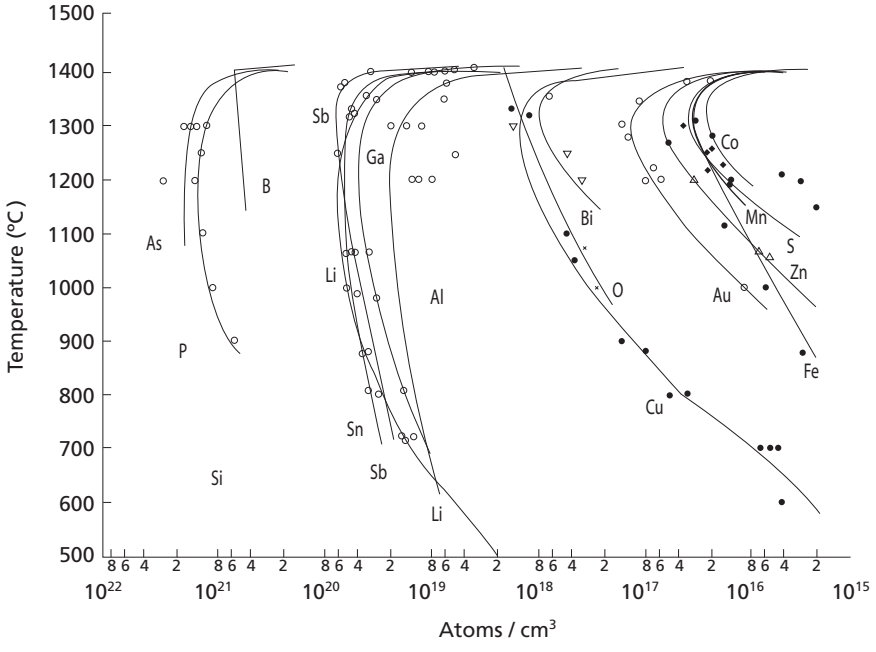

Figure 1. Solid solubility in silicon (Dietl 1983, p. 145).

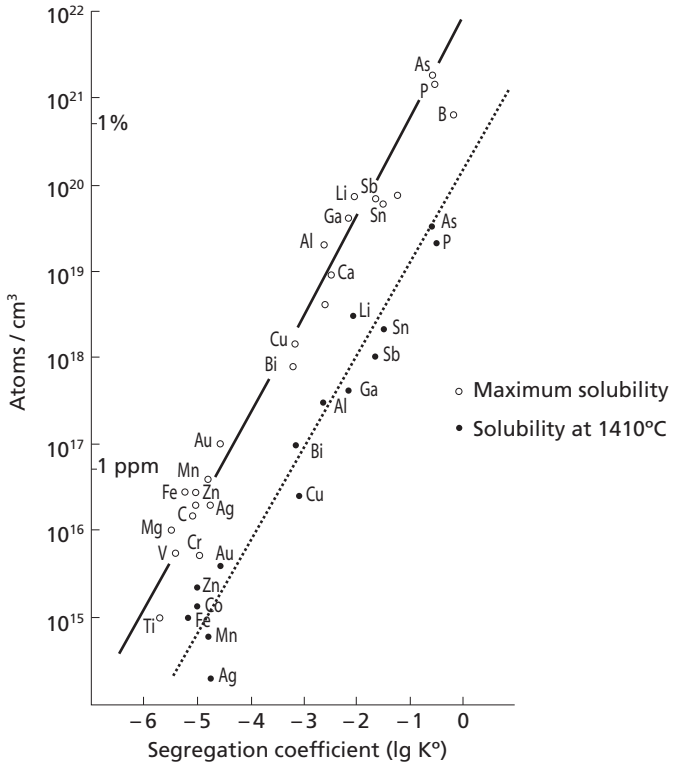

Figure 2. Correlation of solid solubility and segregation coefficient for different impurities in silicon (Dietl 1983, p.145).

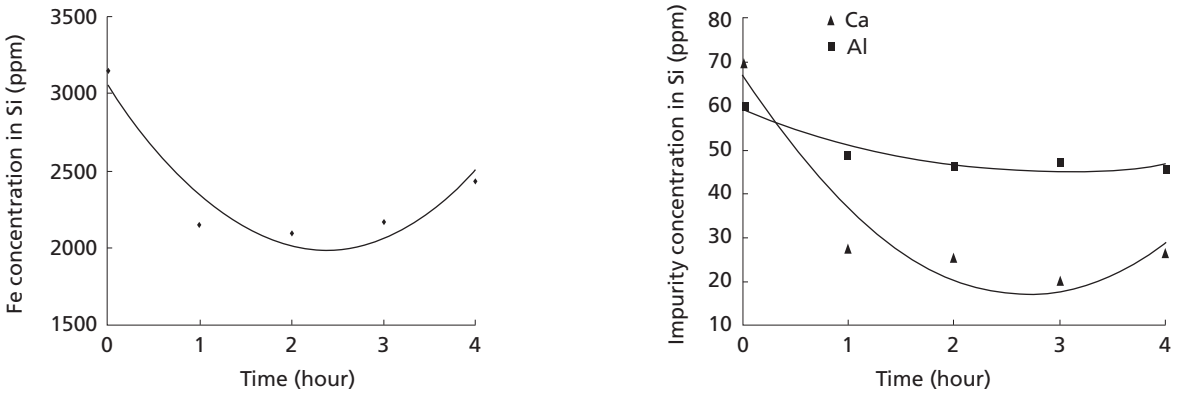

Figure 3. The effect of leaching time on the removal of impurity.

It could be seen that the leaching time of 2 h was suitable for iron and 3 h for calcium removal; but in the case of aluminum, time did not have a significant effect on the removal of Al. As aqua regia is a very strong oxidizing agent, Al particles were surrounded with an oxide layer and the leaching solution had no more effect on the removal of Al after about 1 h.

In Figure 4, the effect of leaching temperature on the removal of impurities is shown. Samples were leached with aqua regia for 3 h and with a liquid:solid ratio of 10:1.

A decrease in the purification of iron was observed at higher temperatures, while an increase was seen in the

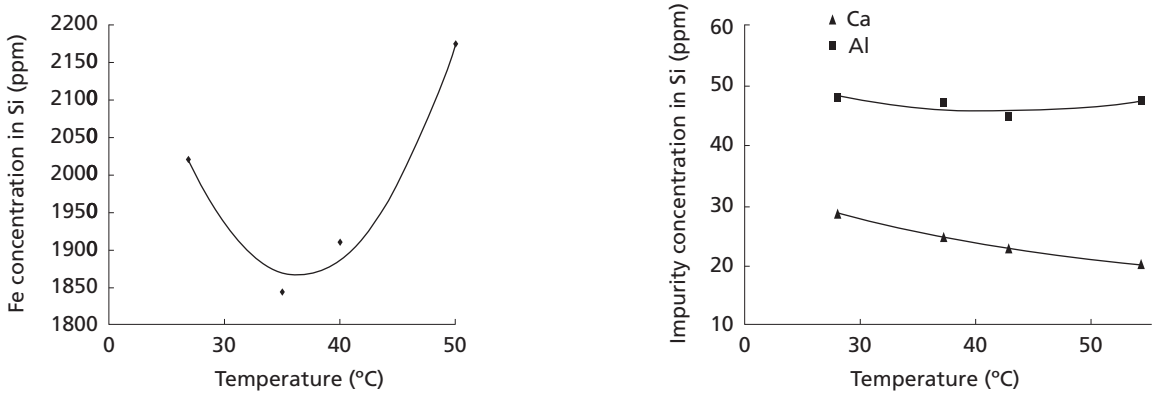

Figure 4. The effect of leaching temperature on the removal of impurity.

removal of calcium at higher temperatures; but in the case of Al, increase of temperature had no significant effect on the purification of silicon.

Etching Effects

To determine the effect of etching on silicon purification, an experiment was done with aqua regia (50ºC, liquid/solid of 10/1, 3h) and prior to leaching; samples were etched with hydrofluoric acid and the results are shown in Table 3.

The results showed that, silicon etching had a positive effect only on the removal of Al from silicon. As mentioned earlier, Al particles were surrounded and covered with an oxide layer and the treatment of silicon with HF generated H_3AlF_6 complex and this dissolved the oxide layer and improved the removal of Al.

Table 3. The effect of preliminary etching on the purification of silicon.

Element	Impurity concentration in Si (ppm)	
	Without etching	With etching
Fe	2174	3001.6
Ca	20.4	40.6
A1	47.6	28

CONCLUSION

An effective leaching time of 2 h and 3 h was obtained for the removal of iron and calcium, respectively, but in the case of aluminum, time had no significant effect on the removal of Al.

Aqua regia is a very strong oxidizing agent, thus during leaching, Al particles were surrounded with an oxide layer and the leaching solution had no effect on the removal of Al after about 1 h.

At higher temperatures, a decrease in the purification of iron was observed, while an increase was seen in the removal of calcium at higher temperatures. In the case of Al, increase in temperature had no significant effect on the purification of silicon.

Silicon etching had a positive effect only on the removal of Al from silicon because treatment of silicon with HF generated H_3AlF_6 complex and this dissolved the oxide layer and improved the removal of Al.

To remove all harmful impurities from silicon, a combination of several refining processes will be needed. This is because of the different behaviour and their characteristics of the various impurities present.

Date of submission: December 2006
Date of acceptance: May 2007

REFERENCES

Dietl, J 1983, 'Hydrometallurgical purification of metallurgical grade silicon', *Solar Cells,* vol. 10, no. 2, pp. 145–154.

Habashi, F 1997, *Handbook of extractive metallurgy,* vol. IV, Wiley–VCH.

Hunt, LP, Dosaj, VD, McCormick, JR & Crossman, LD 1976, 'Purification of metallurgical grade silicon to solar grade quality', in *Proceedings of Solar Energy, Proc. Int. Symp.,* Electro-chemical Society, New York, p. 200.

Lian, SH, Kammel, R & Kheiri, MJ 1992, 'Preliminary study of hydro-metallurgical refining of MG-silicon with attrition